Experimental characterisation of railway wheel squeal occurring in large radius curves

Daniël J Fourie [1,2], Petrus J Gräbe[1], P Stephan Heyns[3] and Robert D Fröhling[2]

[1]University of Pretoria, Transnet Freight Rail Chair in Railway Engineering, South Africa

[2]Transnet Freight Rail, South Africa

[3]University of Pretoria, Department of Mechanical and Aeronautical Engineering, South Africa

Corresponding author: Danie Fourie, University of Pretoria, Chair in Railway Engineering and Transnet Freight Rail, South Africa, Email: danie.fourie4@transnet.net

Abstract

Tonal squeal noise (i.e. the high amplitude singing of a railway wheel with pure tone components) is emitted by some trailing inner wagon wheels on heavy haul trains in 1000 m radius curves on the iron ore export line in South Africa. Field measurements have shown that the trailing inner wheels that squeal are subject to predominantly longitudinal creepage with little to no lateral creepage. The longitudinal creepage acting at the contact of the squealing wheels exceeds 1%, which supports the likelihood of creep saturation and subsequently squeal due to unsteady longitudinal creepage in the large radius curves. Experimental modal analysis of the wheel types identified to be relevant to squeal has revealed that for each unstable frequency, two eigenmodes are likely to be important: one which has a large mode shape component at the wheel-rail contact in the circumferential direction and another which has a large mode shape component at the wheel-rail contact in the radial direction. A frictional self-excitation mechanism based on mode-coupling is favoured as being responsible for squeal excited in large radius curves.

Introduction

In South Africa a noise ordinance exists between Transnet Freight Rail and the community of Elands Bay due to squeal being emitted by some wagon wheels on heavy haul iron ore trains in the 1000 m radius curves passing through the town. The squeal noise in the 1000 m radius curves occurs in the frequency range between 3500 Hz and 7000 Hz and can exclusively be attributed to the trailing inner wheel of bogies underneath empty wagons.[1] The findings of Fourie[1] are explored in greater detail in the next section of this paper. In addition to squeal occurring in the 1000 m radius curves passing through Elands Bay, the author has also observed squeal on the heavy haul line in curves of radii

exceeding 1000 m. Squeal occurring in curves with radii of this magnitude is unheard of in literature and generally occurs exclusively in tight curves of radii smaller than 300 m. [2, 3]

This paper presents an experimental study of the key parameters that influence self-excitation of railway wheels in large radius curves. The study aims to establish a complete experimental characterisation of the phenomenon of squeal occurring in large radius curves. The main parameters that are investigated include, but are not limited to the kinematic parameters and wheel dynamics influencing the generation of squeal in the 1000 m radius curves.

The study also includes finite element modal analysis to ascertain if the wheel modes identified as being involved in squeal have significant out-of-plane vibration that can be linked to the high noise levels associated with squeal.

Modelling the mechanism of self-excitation responsible for squeal occurring in large radius curves falls beyond the scope of this paper and will be the subject of future research. However, the most prominent challenge in modelling the phenomenon is dealt with in this paper, namely to identify the parameters that would warrant self-excitation of the wheels.

Curve squeal

Curve squeal is an instability phenomenon that results from the unstable response of a railway wheel subject to large creep forces in the region of contact between the wheel and rail. The instability is caused by the slip velocity dependent falling friction characteristic of the wheel-rail contact and/or modes coupling of the wheel between different degrees of freedom in the wheel-rail contact.[4] Predominantly, squeal is excited at the leading inner wheel of a four wheeled bogie subject to large lateral creepage, the squeal frequency corresponding to one of the wheel's axial modes of vibration. Most theoretical squeal models in literature account specifically for squeal due to unstable lateral creepage excited at the leading inner wheel.[4-9]

Although the leading inner wheel accounts for most occurrences of squeal, in practice squeal is also excited at the other wheels of a four wheeled bogie.[1, 3, 10-13] Some researchers have extended the common lateral creepage models to include creepage in the longitudinal and spin directions, attempting to account for squeal occurring at other wheels.[14, 15] Such models have however generally been unsuccessful to account for squeal excited at wheels other than the leading inner wheel. Thompson and Monk-Steel[14] show that the leading outer wheel making flange contact, subject to large spin and lateral creepage, is most likely to squeal in its radial modes. However, flange contact has generally been found to reduce the likelihood of stick-slip due to lateral creepage and that it most likely generates flanging noise.[2] Huang et al.[15] demonstrate that the trailing wheels in a tight curve subject to large longitudinal creepage, but small lateral creepage, are unstable in their fundamental circumferential mode. The wheel model used in the study of Huang et al.[15] consisted of a full wheelset and the fundamental circumferential mode occurred at 70 Hz.   Because the fundamental

circumferential mode generally occurs between 50 Hz and 100 Hz, longitudinal creepage is not considered relevant to squeal.[16] Instead longitudinal creepage is believed to be relevant to corrugation formation. Rudd[5] also discredits longitudinal creepage and wheel flange rubbing as mechanisms for squeal based on the hypothesis that the excitation forces associated with longitudinal creepage and wheel flange rubbing excite the wheel in its own plane where it is a relatively inefficient radiator of sound. On the other hand lateral creepage excites the wheel normal to its plane where it is an efficient radiator of sound. In reality the wheel's modeshapes contain coupled in-plane and out-of-plane motions. This is different to Rudd's hypothesis for discounting longitudinal creepage and flange rubbing as squeal mechanisms.

Based on the above, the conclusion can be drawn that researchers studying squeal are in agreement that unsteady lateral creepage is the dominant cause for squeal generation whilst longitudinal creepage and flange rubbing are not considered relevant to squeal. Based on this conclusion the author conducted a wayside measurement campaign at Elands Bay based on the hypothesis that the impaired curving ability of self-steering bogies, and curving with excessive lateral creep forces/angles-of-attack, is responsible for the generation of squeal noise in the large radius curves.[1] The results of this measurement campaign in terms of the simultaneous measurement of sound pressure levels and lateral wheel-rail forces subsequently proved this hypothesis invalid. Instead the results proved that whilst some squeal events emanated from bogies curving with higher lateral forces than expected for the curve, most of the squeal events emanated from bogies curving with lateral forces close to that expected for the 1000 m radius curve. In neither of the instances the lateral forces were high enough to lead to saturated lateral creep conditions.

The measurement results did however prove that the squealing in the 1000 m radius curve can be exclusively attributed to the trailing inner wheel of some bogies under empty wagons and that the squealing bogies all curved with the same distinct curving signature. The specific local contact conditions of the squealing wheel could however not be uniquely identified without knowing the lateral displacement of the trailing wheelset with respect to the inner and outer rails of the curve. The curving signature could be interpreted as either the trailing inner or trailing outer wheels making flange contact. If the trailing outer wheel is identified as making flange contact, the trailing inner wheel is subject to predominantly longitudinal creepage given the near radial alignment of the wheelset. Otherwise the trailing inner wheel is subject to flange throat/rail gauge corner contact. The current research is a continuation of the previous research by Fourie[1] and aims to broaden the understanding of the parameters and mechanisms influencing squeal generation in large radius curves.

Research Methodology

The field measurements for the current research use a modified measurement setup compared to that of Fourie[1]. The modification consists primarily of the inclusion of laser triangulation sensors to measure the lateral wheelset displacement within the available flangeway. The complete

measurement setup and the evaluation of such field measurements are explored in detail in the following two sections.

In addition, the modified measurement campaign identified the wheel diameter and wheel type of the squealing wheels from the recorded vehicle identification numbers. The field measurements in the test curve using the modified set-up aimed to qualify the source of squeal, the squeal frequencies and the creepages present in the wheel-rail contact of the squealing wheel as well as to establish a correlation between wheel types, wheel diameter and squeal frequency. Wheel types of three different manufacturers are used. The above field measurements formed phase 1 of the current investigation.

The second phase was concerned with identifying the wheel eigenmodes involved in squeal and establishing a relationship between the kinematic parameters found to be important to squeal and such eigenmodes.

The third phase was concerned with determining if the wheel modes identified as being involved in squeal have significant out-of-plane vibration that can be linked to the high noise levels associated with squeal.

Field measurements

Measurement setup

For the study of curve squeal in a 1000 m radius curve, a measurement methodology was developed to identify the frequency of squeal, the source of squeal i.e. the exact wheel in a bogie that the squeal originated from, the steady state curving attitude of the bogie as well as the creepages present in the wheel-rail contact of the squealing wheel.

The measurement setup consisted of two free field microphones located at 7.5 m from the track centre on either side of the track and radially aligned with a set of strain gauge bridges configured to measure the lateral and vertical forces on the low and high rail of the curve. This set-up allows the squealing wheel to be identified from the magnitude difference of the sound pressures recorded by the inner and outer microphones in combination with comparing the point of frequency shift of the squeal event due to the Doppler Effect with the simultaneously sampled force signals of the radially aligned strain gauge bridges.[1] The web chevron and base chevron strain gauge configurations were used respectively for the measurement of vertical and lateral rail forces.[17] In addition two laser triangulation sensors were used to measure the lateral displacement of the wheelset within the available flangeway.

The vertical force signals also provided impulse signals that could be used to determine the wagon speed and thus the speed profile for each recorded train. Only trains with a constant or increasing speed profile past the measurement location were considered for the subsequent analysis. Trains

with mechanical brakes being applied were not considered in the subsequent analysis as squeal due to braking could distort the noise signal.

Figure 1 shows a simple schematic of the test setup. All data was recorded using a sampling rate of 40 kHz.
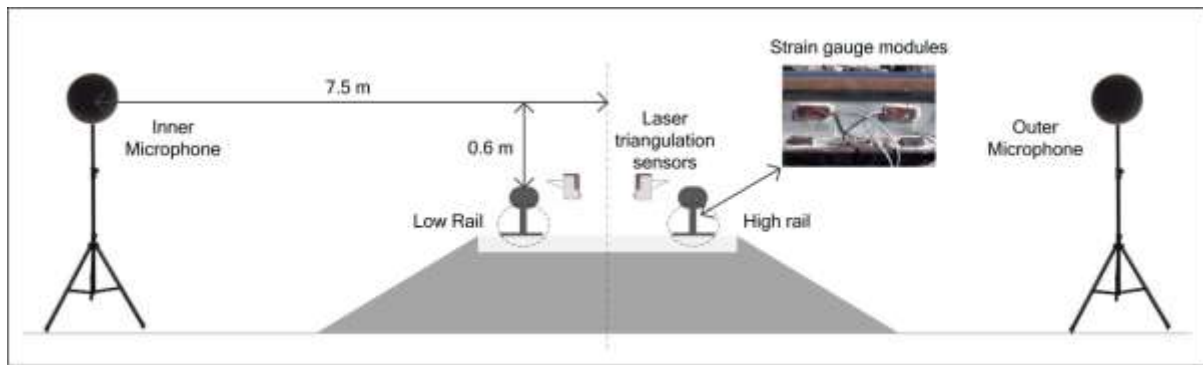

Figure 1. Test setup at Elands Bay.

Vehicle identification numbers and orientations of the recorded trains were obtained after the measurement campaign via Transnet's train condition monitoring database. This allowed the squealing to be attributed to a specific wheel of a specific wagon. Knowing the exact wheel which emitted the squeal event allowed for obtaining the wheel diameters of the squealing wheels, also available in the train condition monitoring database via the wheel profile monitor located on the line. The vehicle numbers and orientations were also used later to manually identify the wheel type of the squealing wheels from a slow speed video recording of trains leaving the departure yard.

Evaluation of field measurements

Source of squeal. The combined study of the time-dependent frequency spectra, the sound pressure levels as well as the signals from the radially aligned strain gauge bridges enabled the identification of the source of squealing. Time dependent linear frequency analysis revealed how the frequency of a passing train changes over time, whilst equivalent continuous sound pressure levels in 1/8 second intervals revealed the true time history of the passing train.

The time-dependent frequency spectra of the recorded sound pressure showed characteristics due to the Doppler Effect when squealing wheels passed the microphone location (see Figure 3(a)). This implies an increase or decrease of the frequency observed by the stationary device depending on the direction of relative movement of the source.

By comparing the point of frequency shift of the squeal event due to the Doppler Effect with the simultaneously sampled force signals of the radially aligned strain gauge bridges, the source of the

squeal could be identified along the length of the train. The peaks of the measured forces on the rail indicate the exact time that a wheel passed the measurement location. A similar technique (using the Doppler Effect) was employed by Stefanelli et al.[18] to detect the squealing source along the length of the train.

The point of frequency shift is determined as follows.

As a first step, the true squeal frequency f_b (line B in Figure 3(a)) is approximated from the observed frequencies before f_a and after f_c the passage of the source (lines A and C respectively in Figure 3(a)) by solving Equations 1 and 2 simultaneously.

$$f_a = \left(\frac{v}{v - v_s}\right) f_b \tag{1}$$

$$f_c = \left(\frac{v}{v + v_s}\right) f_b \tag{2}$$

In Equations 1 and 2 v is the speed of sound in air (343 m/s at 20°C) and v_s the source speed.

This time dependent linear frequency analysis is a compromise between resolution in the frequency domain and resolution in the time domain. For this analysis a window length of 16384 samples was chosen giving a frequency resolution of 2.44 Hz and a time resolution of 409.6 ms. This enables the required frequency resolution to accurately determine the squeal frequencies.

Solving Equations 1 and 2 simultaneously also yields an estimate of the wagon/source speed. To gain additional confidence in the estimated real squeal frequency, the estimated speed was compared to the true speed of the wagon. See Figure 2.
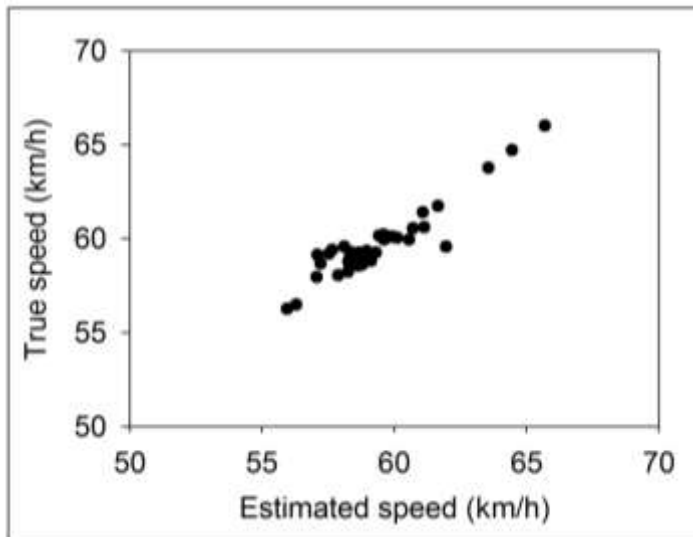

Figure 2. Estimated wagon speed vs. true wagon speed.

Secondly, the instantaneous time that the squealing wheel passes the microphone location (line D in Figure 3(a)), also known as the point of frequency shift, is determined by the point where the squeal frequency line crosses the Doppler curve. For this analysis a window length of 1024 samples was chosen, giving a frequency resolution of 39.06 Hz and a time resolution of 26 ms. This enables the required time and frequency resolutions to accurately determine the point of frequency shift for wagons travelling at between 50 km/h and 70 km/h, resulting in a passing time between wheelsets in a bogie of between 132 ms to 94 ms.

For both the first and second stages of the point of frequency shift analysis, it is important to select the amplitude range for colour coding the amplitude of the frequency content such that the Doppler curve can be clearly distinguished from the surrounding frequency content in the time-frequency plot.
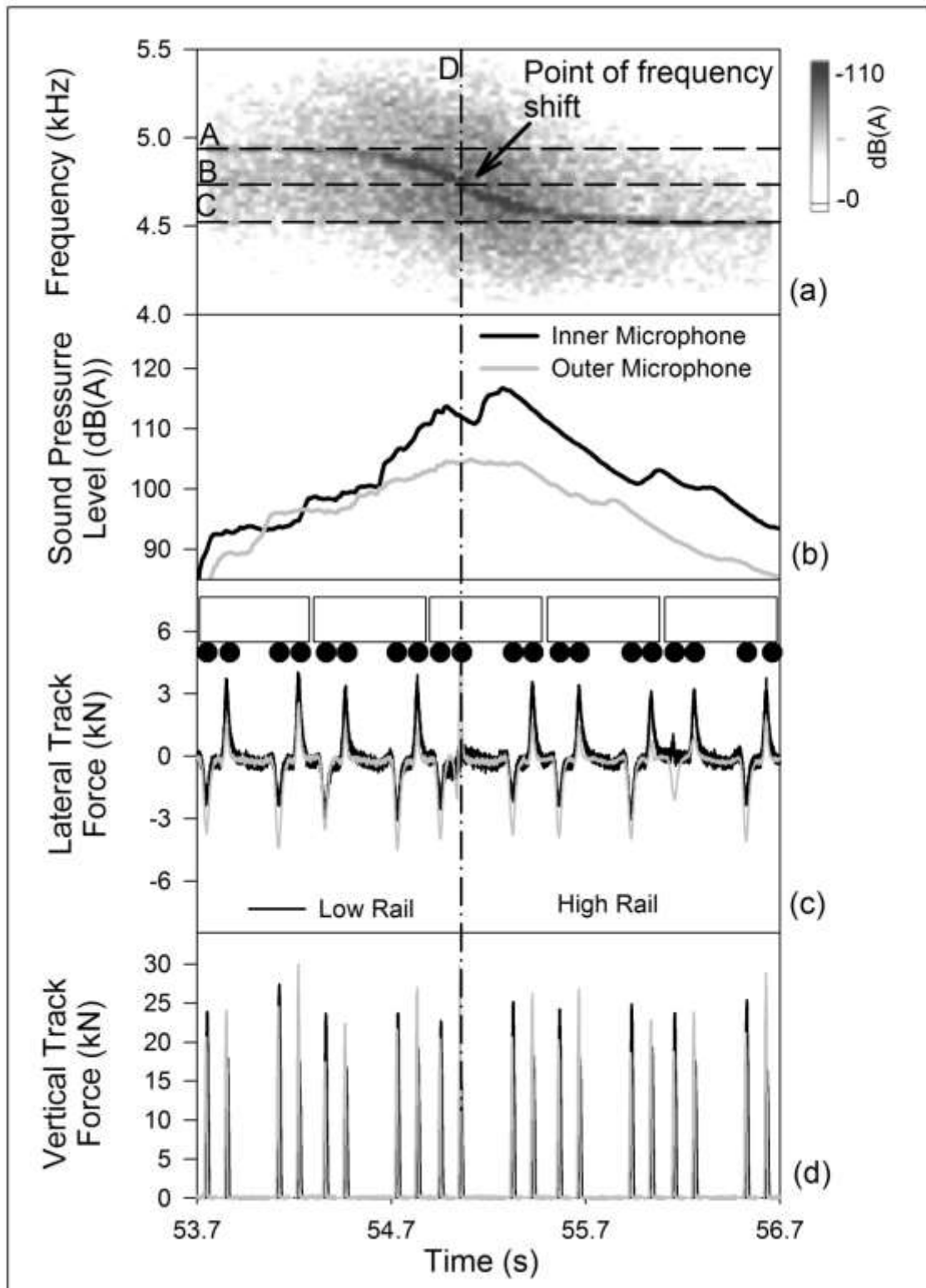
Figure 3. Identification of squealing wheel from simultaneously measured sound pressure and lateral forces: (a) Time-dependent frequency spectra showing Doppler Effect. (b) Sound pressure level recorded by inner and outer microphones. (c) Lateral force signals from strain gauge bridges. (d) Vertical force signals from strain gauge bridges.

Comparing the sound pressure level difference between the inner and outer microphones allows identification of the side of the train that the squeal event originated from. Evident from figure 3(b) is that the point of frequency shift doesn't coincide with the maximum sound pressure level due to squeal. This can most likely be attributed to the directivity of wheel radiation. The measured sound pressure generally has a minimum on or close to the axis of the wheel due to cancellation between the contributions from different parts of the mode shape[2].

Combining the point of frequency shift analysis with the sound pressure level difference analysis, yield the exact wheel in a bogie that the noise event originated from. It is evident from Figure 3 that this squeal event originated from the second axle of the third wagon and from the wheel in contact with the low rail.

Similar to Fourie[1], results from the current measurement campaign also proved that squeal in the large radius test curves can be uniquely attributed to the trailing inner wheel of a bogie in contact with the low rail.

To gain confidence in the source identification technique described above the position of the closest wheelset to the squealing wheelset is shown in Figure 4.
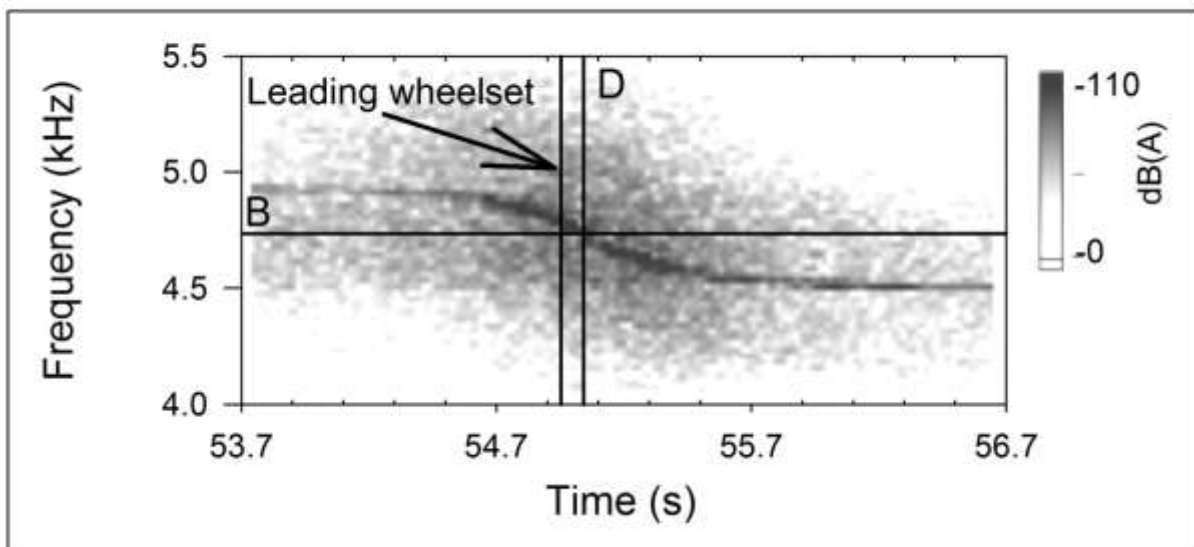

Figure 4. Position of leading wheelset with respect to Doppler curve

This technique for identifying the frequency shift from the Doppler Effect in time-frequency curves is limited to squeal events that occur sufficiently far from one another in the time or frequency domains so that the Doppler curves do not interfere with one another. For squeal events that occurred close to one another in the time domain with closely matched squeal frequencies this technique shows limited

success. The vast majority of squeal events for the 342 wagon long trains had sufficient spacing in the time domain ensuring the success of the described technique.

If the squeal events occur close to one another in the time domain, but sufficiently far apart in the frequency domain, then band pass sound pressure filtering should be used to distinguish if the squeal events originated from the inner or outer wheels.

Bogie curving characteristic. The measurement of lateral track forces on curved track, combined with information on the condition of rolling stock can provide valuable information about the curve negotiation characteristics of bogies. The lateral force curving signature not only reveals the levels of wheel-rail forces required for bogie curving, but also whether the bogie is curving by means of creep forces generated at the wheel-rail interface only or if contact is necessitated between the wheel flange throat and rail gauge corner to help steer the bogie around the curve. Wheel flange throat/rail gauge corner contact can be confirmed by additional measurement of the wheelset lateral displacement within the available flangeway.

Lateral force curving signatures for a bogie underneath an empty wagon and representative of curving by means of creep (frictional) forces (C) only, with the leading outer wheel in flange contact as well as both the leading and trailing outer wheels making simultaneous flange contact are presented in Figure 5. Flange contact results in flange and spin creep forces and are denoted by the letter F in Figure 5. These three curving characteristics can be used to describe the curving behaviour of the most bogies underneath empty wagons in the 1000 m radius test curves.

The black dots in Figure 5 represent the lateral wheelset displacement measurements. Lateral wheelset displacement from the track centre towards the high rail is given a positive convention, whilst displacement towards the low rail is given a negative convention. In addition the available flangeway clearance is also indicated in the figure.
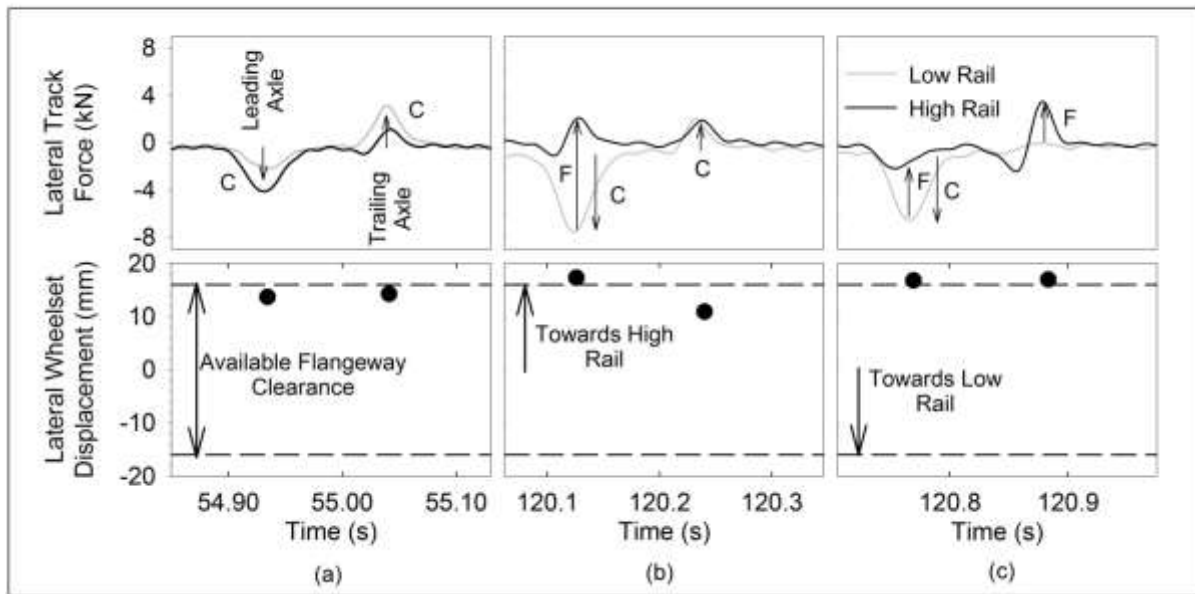
Figure 5. Lateral force curving signatures: (a) Curving solely utilising creep forces. (b) Flange contact of leading outer wheel. (c) Flange contact of leading and trailing outer wheels.

Curving solely by means of creep forces (see Figure 5(a)) occurs with a positive angle of attack (AoA) of the leading wheelset and a negative AoA of the trailing wheelset of a two axle bogie. Using the convention of a positive lateral force to the outside of the curve for both the high and low rails, curving by means of only creep forces will result in lateral track forces acting towards the inside of the curve for the leading wheelset and lateral track forces acting towards the outside of the curve for the trailing wheelset. Both wheelsets displace an equal distance towards the outer rail due to the steering mechanism of the wheelsets in a curve.

Once a bogie has lost its ability to steer around a curve using only creep forces, the flange or flange throat of the leading outer wheel comes into contact with the gauge corner of the high rail to steer the bogie. Subsequently, flange contact and high levels of spin creepage, that are associated with wheel-rail contact occurring at high contact angles between the rail gauge corner and the wheel flange throat, result in a lateral force opposing the lateral force component due to lateral creep. The resultant lateral force of the leading wheelset thus becomes less negative or even positive on the high rail while the lateral forces on the low rail remain largely unchanged (see Figure 5(b)). Flange and spin creep forces (F) act in a direction opposite to the lateral creep forces (C).

Under certain conditions the flange of both the leading outer and trailing outer wheels of a bogie can be in flange contact as shown in Figure 5(c). This implies that both wheelsets of the bogie are displaced towards the high rail taking up all the available flangeway. All squealing bogies took on this curving attitude. A substantial number of bogies taking on this curving attitude and not squealing could also be identified from the measurements.

11

Creepages present in wheel-rail contact of squealing wheel. Judging from the curving characteristic of the squealing bogies, the creepages present at the wheel-rail contact of the squealing wheels can be deduced.

First of all, from the close to zero lateral force acting on the trailing inner wheel of the bogie curving signature in Figure 5(c), it can be deduced that the trailing wheelset is curving radially aligned with the centre of the curve. This implies the trailing wheelset is curving with a near zero AoA and that the trailing inner squealing wheels are subject to little to no lateral creepage.

The magnitude of the quasi static longitudinal creepage λ_x acting on the trailing inner squealing wheels can be estimated using Equation 3 and knowing the rolling radius difference Δr vs. lateral displacement y functions of the squealing wheelsets. Δr_{1000m} is the rolling radius difference required to achieve free rolling of a wheelset in the 1000 m radius test curve which is 0.53 mm, r_0 is the wheel radius at the taping line of the wheel. Δr to achieve free rolling was calculated using Equation 4 with a wheel radius r_0 of 458 mm and a wheelset taping-to-taping line distance, l, of 1152 mm.

$$\lambda_x = {(\Delta r - \Delta r_{1000m})}/{r_0} \tag{3}$$

$$\Delta r_{1000m} = {r_0 l}/{1000000} \tag{4}$$

The rolling radius difference vs. lateral displacement (Δr vs. y) functions of the squealing axle's wheel profiles and the matching test curve high and low rail profiles were determined using the kinematic simulation software RsGeo[19]. The wheel and rail cross sectional profiles were measured using MiniProf wheel and rail profile tracers.

Figure 6 shows such Δr vs. y functions for four squealing wheelsets on the test curve rails. The squealing wheelsets in the figure are identified by the respective wagon number. Also shown in the figure is the Δr vs. y function for a wheelset having the design No 21 Transnet Freight Rail wheel profiles making contact with the measured rail profiles. A positive lateral displacement as indicated implies a lateral displacement away from the track centre towards the high rail in a curve.
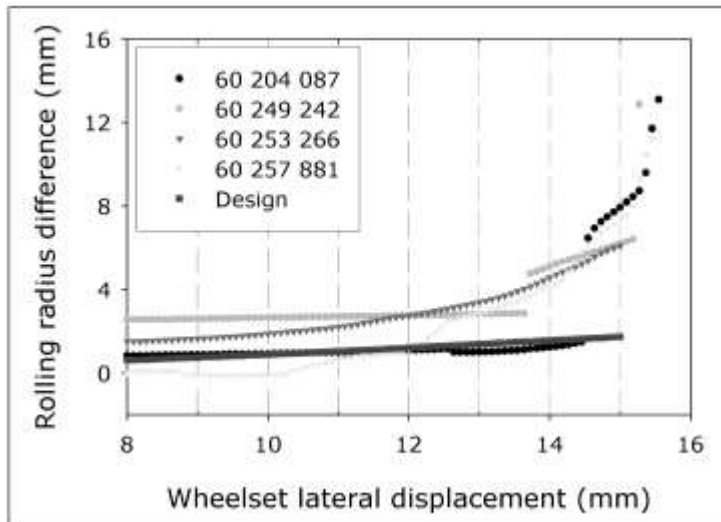
Figure 6. Δr vs. y functions of squealing wheelsets.

For a track gauge of 1071 mm, a wheelset back-to-back distance of 987 mm and the wheels profiled to No 21 profiles, flange contact occurs approximately at a wheelset lateral displacement of 15 mm. It is evident from Figure 6 that the rolling radius difference for all of the squealing wheelsets exceeds 6 mm at 15 mm lateral displacement. Assuming a 916 mm diameter wheel, a 6 mm rolling radius difference translates to a longitudinal creepage of 1.2%.

For a typical friction characteristic at the wheel-rail interface creep saturation occurs at about 1% creepage.[20, 21] The rolling radius differences in excess of 6 mm prove the possibility of creep saturation and subsequently squeal due to unsteady longitudinal creepage to occur in the large radius test curves.

It is also evident from Figure 5(c) that the leading inner wheel could have high levels of longitudinal creepage acting at the wheel-rail contact. In addition the leading inner wheel also exhibits a high lateral force which implies lateral creepage. The leading inner wheel has not been identified as squealing in the test curves. A possible explanation for this could be that lateral creepage suppresses squeal due to unsteady longitudinal creepage similar to the study of Monk-Steel et al.[22] that showed how longitudinal creepage suppresses the formation of squeal due to unsteady lateral creepage.

Squeal frequency versus wheel diameter.

A plot of the identified squeal frequencies and wheel diameters for the three different wheel types are presented in Figure 7.

An estimation of the frequency before and after the passage of the source based on time-frequency plots similar to Figure 3(a) leads to an approximate squeal frequency, solving Equations 1 and 2

simultaneously. Wheel diameters were assessed statistically as the median of measurements stretching over a two month period, allowing for outliers due to measurement anomalies to be excluded from the data set.

The wheels start off at a diameter of 916 mm and are progressively machined down to maintain an acceptable wheel profile. The minimum allowed wheel diameter is 870 mm. The wheel types are denoted as types A, B and C.
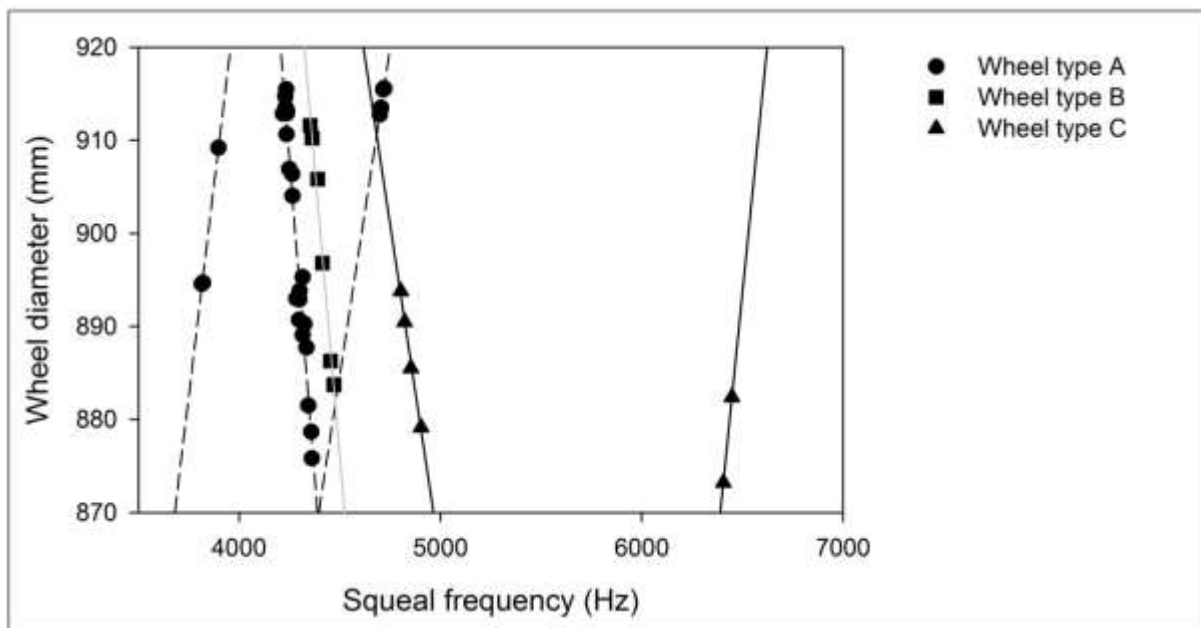

Figure 7. Squeal frequency vs. wheel diameter for three wheel types used on line.

Figure 7 shows how the measured squeal frequencies of the different wheel types change over the lifespan of the wheel. It is evident from Figure 7 that for wheel type A, three unstable modes can be identified from the measurement results. These are possibly related to three distinct eigenmodes of the wheel. The existence of three unstable modes for wheel type A becomes evident from the linear variation of the measured squeal frequencies against wheel diameter for three distinct linear varying sets of data points associated with wheel type A. This has been highlighted in Figure 7 with three dashed black linear regression lines. For wheel type B, only one unstable mode can be identified as shown by the solid grey linear regression line. For wheel type C, two unstable modes can be identified as highlighted by the solid black regression lines.

The results also prove that the wheels retain the ability to squeal over their entire lifespan. The reason that squeal for wheel type C was only observed at smaller wheel diameters can be attributed to this wheel type currently being phased out from the ore line i.e. no new type C wheels are being introduced on the line and the existing wheels are allowed to be progressively machined down to 870 mm diameter.

Wheel eigenmodes involved in squeal

The study of the wheel eigenmodes involved in squeal were conducted via modal analysis of wheel types A and B of known diameter (916 mm) and mounted underneath an empty ore wagon. The point and cross receptances (displacement per unit force as function of frequency) were also characterised for wheel types A and B for the same mounted wheelsets freely suspended.

Modes of vibration of a railway wheel

The modes of vibration of a railway wheel can be characterised by a number of nodal diameters n and nodal circles m. These nodal diameters and circles can occur in any combination for the in-plane and out-of-plane motion. The railway wheel sustains out-of-plane motion through its axial modes, whilst in-plane motion is sustained through its radial – or circumferential modes. Because of the asymmetry of a railway wheel's cross section the in-plane and out-of-plane motions become coupled.

Figure 8(a) to Figure 8(c) show some examples of the zero-nodal-circle axial, radial and circumferential mode shapes, whilst Figure 8(d) introduces the concept of nodal circles by showing some examples of one-nodal-circle axial modes. It is left to the reader to deduce the effect of more nodal circles on the axial, radial and circumferential mode shapes of a wheel. Positive and negative signs indicate the relative phase of vibration in the different areas of the wheel. For the axial modes in Figure 8(a) the vibration is normal to the area, for the radial modes in Figure 8(b) the vibration is normal to the periphery whilst the vibration is tangential to the wheel periphery for the circumferential modes in Figure 8(c).
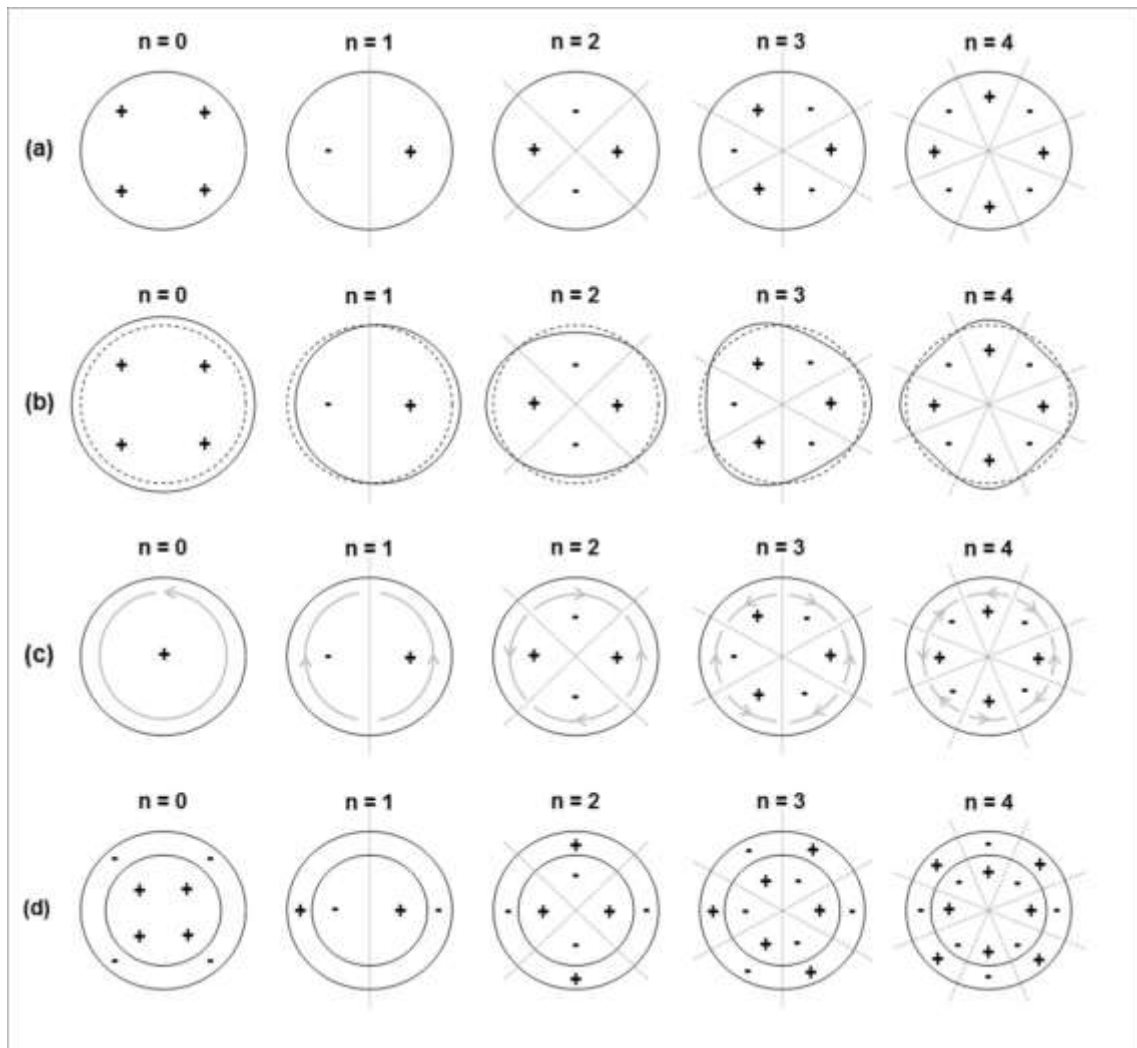
Figure 8. Wheel eigenmodes: (a) Zero-nodal circle axial modes. (b) Zero-nodal-circle radial modes (--- undeformed shape, — deformed shape). (c) Zero-nodal-circle circumferential modes. (d) One-nodal-circle axial modes.

For each mode shape with one or more nodal diameters, the mode shapes occur as spatially orthogonal pairs, with the nodes becoming the anti-nodes in the other, and vice versa. These are two independent modes with the same or slightly different resonant frequencies whose mode shapes in the circumferential direction are described by the forms $A \sin n\theta$ and $A \cos n\theta$ respectively. θ is the circumferential angular coordinate and A is a function of the radial, axial and circumferential coordinates. As an example, see Figure 9 illustrating the two-nodal-diameter orthogonal axial mode pair.
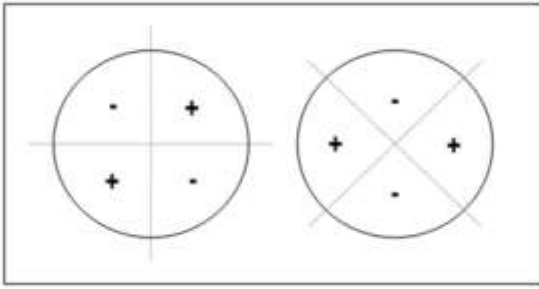
Figure 9. Two-nodal-diameter spatially orthogonal axial mode pair.

For a wheel mounted underneath a vehicle, the contact point between the wheel and rail will fix the angular location of the nodal diameters of the mode shape.[10] For mode shapes with $n > 0$, the sine eigenforms align themselves on the wheel in such a way that one of their nodal points agrees with the wheel-rail contact point.

Experimental Modal Analysis

Due to the regular sinusoidal pattern in the circumferential direction for the mode shapes of the wheel, a detailed modal analysis was not deemed necessary to identify the modes of vibration of the wheel responsible for squeal. Instead a reduced approach was followed to study the mode shapes of the mounted wheel.

Firstly, a modal analysis was carried out to identify the sinusoidal pattern of each mode in the circumferential direction around the wheel tread. The measurement grid encompassed 9 measurement points spaced at unequal distances around a quarter of the wheel (see Figure 10).
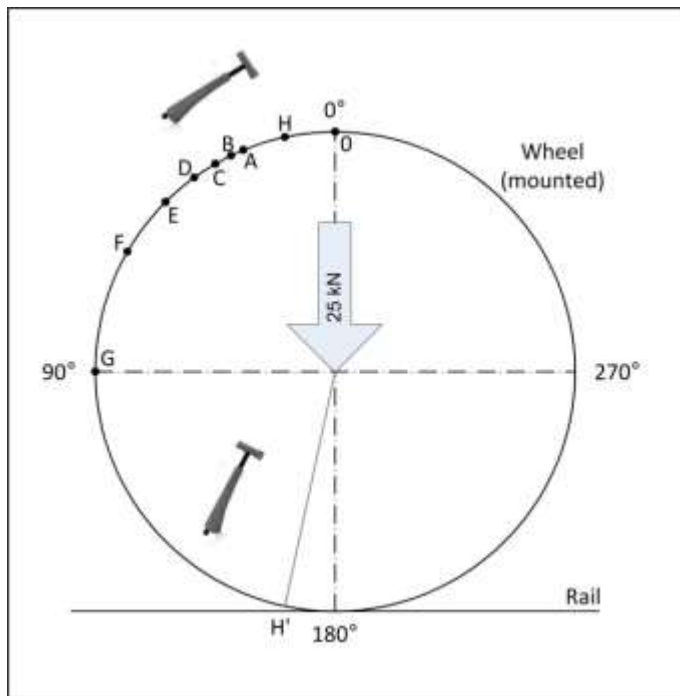
Figure 10. Measurement grid on wheel.

The angular positions of grid points A to G and O were chosen to correspond with nodal diameters of the sine modes with 1 to 8 nodal diameters and aligned to have one of their nodal points at the wheel-rail contact point. Excitation was provided at grid point H, which was selected to not coincide with a nodal diameter of one of the 1 to 8 nodal diameter sine modes. The wheel was excited in both the radial and axial directions at the excitation point.

For the modal analysis an instrumented hammer was used to provide the excitation, and the response was measured using a single tri-axial accelerometer. A roving accelerometer approach was used to capture the wheel mode shape components in the radial, axial and circumferential directions at each measurement point. An average of three impacts was used for each measurement. The response and radial excitation points on the wheel tread were chosen 105 mm from the back of flange to correspond with the average of the contact positions identified for the inner squealing wheels via the results of the RsGeo simulations. The receptance for each input/output location were recorded and were later used to extract the modal parameters of each mode using the least squares exponential curve fitting algorithm available in the Labview environment.

The eigenvectors representative of the different modes were normalised to unit modal mass.

An example of the results for sinusoidal pattern recognition is presented in Figure 11. The results are plotted for the unwrapped rim between 0° and 90°. Because the wheel-rail contact point fixes the location of the nodal diameters the cosine modes could also be identified from the modal analysis.

Figure 11 shows the radial, circumferential and axial mode shape components for the six nodal diameter radial doublet modes occurring at 3942 Hz and 3970 Hz respectively. Evident from the mode shape components is that the above modes have large modal amplitudes in the radial and circumferential directions at the wheel tread.
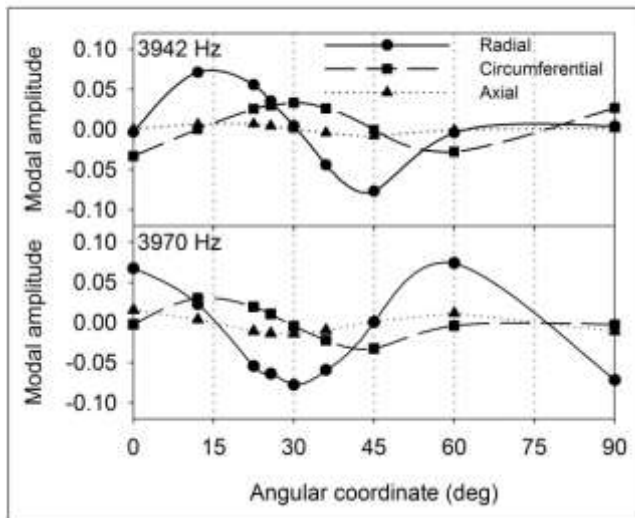

Figure 11. Sinusoidal mode shape components at wheel tread.

Secondly, a modal analysis was carried out on a single cross section of the wheel. The grid points were spaced 25 mm apart and was located at the wheel cross section indicated by H' in Figure 10. By studying the response of a single cross section the number of nodal circles can be judged.

Eigenmodes involved in squeal

Figure 12 shows a comparison between the measured squeal frequencies and the eigenfrequencies of the wheel eigenmodes most likely to be involved in squeal for wheel types A and B at the test curves.

It is evident from Figure 12 that the squeal frequencies associated with wheel type A closely match the eigenfrequencies of (i) the six nodal diameter radial doublet modes, (ii) the two nodal diameter circumferential doublet modes and (iii) the seven nodal diameter radial doublet modes. For a 916 mm diameter wheel, the six nodal diameter radial (6,R) doublet modes occur at 3942 Hz and 3970 Hz, the seven nodal diameter radial (7,R) doublets at 4743 Hz and 4760 Hz and the two nodal diameter circumferential (2,C) doublets at 4249 Hz and 4261 Hz.
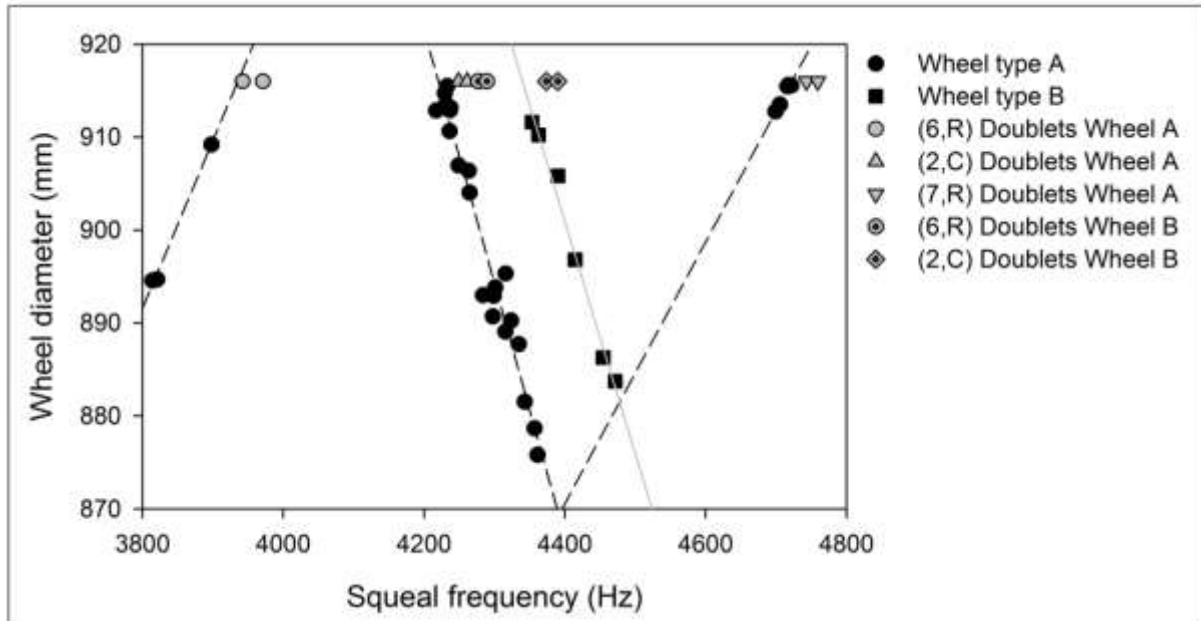
Figure 12. Comparison between wheel eigenfrequencies and squeal frequencies.

In contrast to this, the squeal frequency associated with wheel type B occurs approximately halfway between the sets of eigenfrequencies representing the six nodal diameter radial doublet modes (4277 Hz and 4289 Hz for a 916 mm diameter wheel) and the two nodal diameter circumferential doublet modes (4374 Hz and 4390 Hz for a 916 mm diameter wheel). This behaviour where the unstable frequency of a self-excited frictional system occurs not at an eigenfrequency of the system, but between eigenfrequencies of the system is characteristic of mode-coupling instability where the eigenfrequencies of two structural modes of an undamped system come, as a function of the control parameter, closer and closer together until they coalesce and a pair of a stable and unstable mode results.[23] Negative damping on the other hand renders single structural modes of the system unstable and therefore the squeal frequency correlates with one of the eigenmodes of the damped system.

Based on the locality of the squeal frequency of wheel type B against its closest eigenmodes, a squeal mechanism based on mode-coupling instability with a constant friction coefficient is favoured.

If mode-coupling instability was to be applied to curve squeal excited as a result of the presence of large longitudinal creepage at the wheel-rail interface, it would suggest that the self-excited oscillations are to be caused by the proportionality between the longitudinal creep force and the normal force during sliding as well as structural coupling between the vertical and longitudinal degrees of freedom of the wheel-rail system with respect to the contact.

To understand the degree of frictional coupling that exists between the vertical and longitudinal degrees of freedom (with respect to the wheel-rail contact) for the four cases of instability, consider Figure 13. Figure 13(a) to (d) present the radial and circumferential mode shape components of the mode shapes identified to be relevant to squeal and having an anti-node at the wheel-rail contact

point. The mode shape components in Figure 12 were obtained by fitting a sine curve to the estimated mode shape components. The mode shapes are plotted for an unwrapped rim between 90° and 270° with the contact point occurring at 180° and additionally indicated with an arrow in the figures.
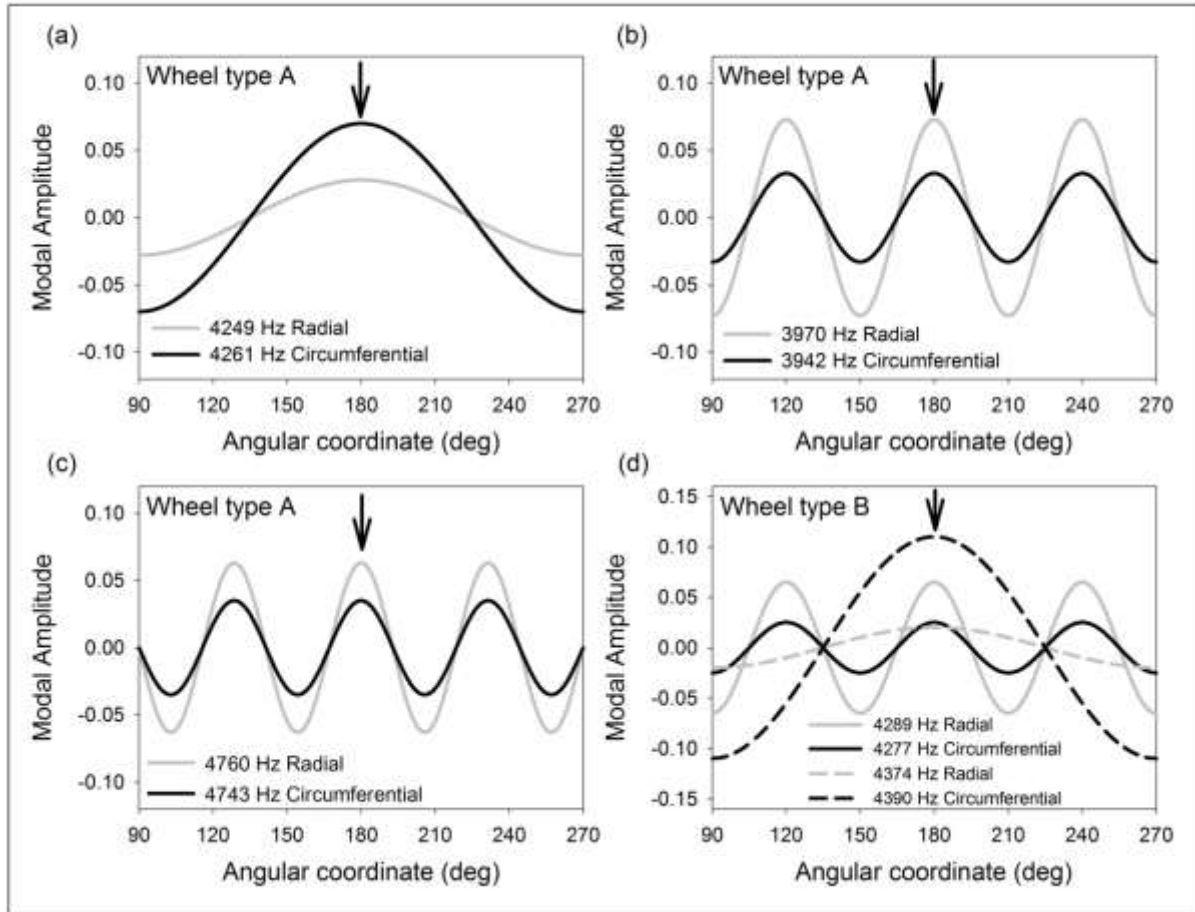

Figure 13. Radial and circumferential mode shape components of eigenmodes most likely to be relevant to squeal.

It is evident from Figures 13(a) to (d) that in all four cases of instability two independent mode shapes, one with a large mode shape component in the radial direction at the wheel-rail contact and another with a large mode shape component in the circumferential direction at the wheel-rail contact could be identified in close proximity to the squeal frequencies. For wheel type A the modes were the independent doublet modes occurring at almost identical frequencies and for wheel type B the modes were the cosine modes of the (6,R) and (2,C) doublet modes respectively.

Furthermore, to understand the degree of structural coupling that exists between the vertical and longitudinal degrees of freedom (with respect to the wheel-rail contact) for the four cases of instability see Figure 14. Figures 14(a) and (b) show the vertical and longitudinal point receptances as well as the vertical/longitudinal cross receptances for wheel types A and B respectively. The response and

impact excitation points were chosen to be 105 mm from the back of the flange. The circumferential impact was provided on a small steel block rigidly fixed to the wheel tread. An average of 30 impacts was used for the calculation of each of the receptances. The squeal frequencies are marked with black arrows in the figure.
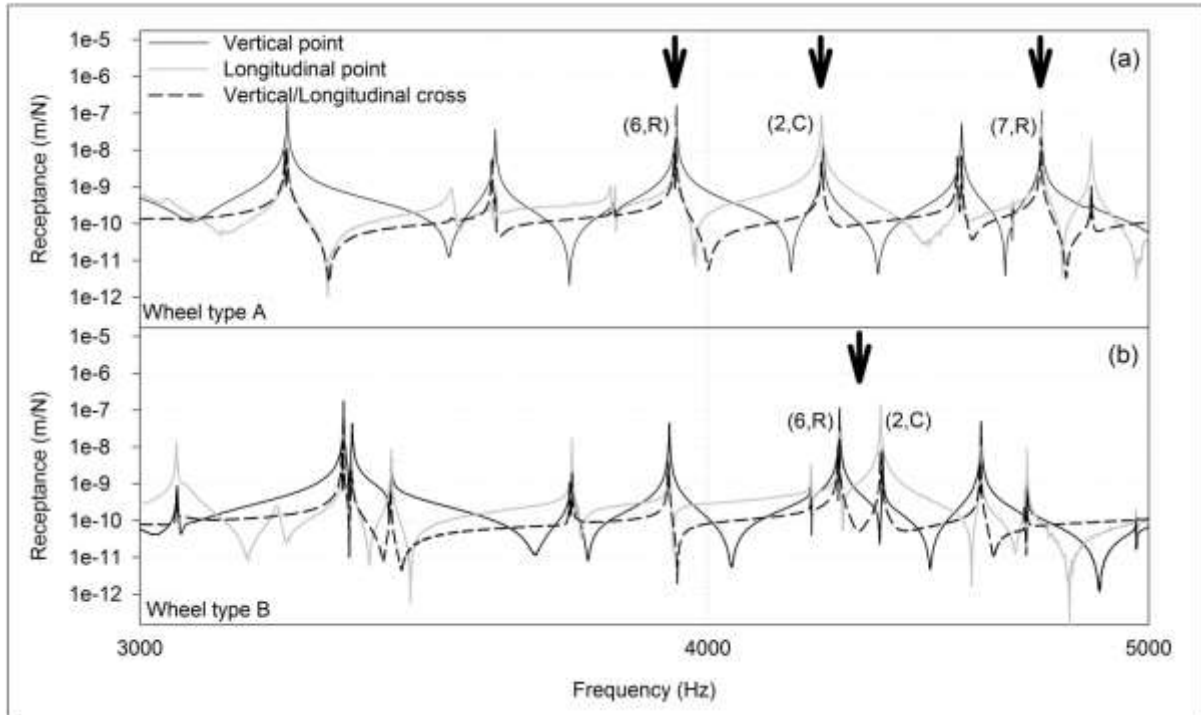

Figure 14. Magnitudes of wheel receptances (Vertical point, Longitudinal point and Vertical/Longitudinal cross) on the tread (a) Wheel type A (b) Wheel type B.

For each of the squeal frequencies of wheel type A and associated with the (6,R), (2,C) and (7,R) doublet modes respectively, strong structural cross coupling exist between the sine and cosine doublet eigenmodes as evidenced by the sharp rise in the vertical/longitudinal cross receptance at these frequencies (see Figure 14(a)). It is important to take note that the sharp rise in the vertical point receptance at the squeal frequencies is associated with the (6,R) and (7,R) sine and (2,C) cosine eigenforms respectively, whilst the sharp rise in the longitudinal point receptance at these frequencies is associated with the (2,C) sine and (6,R) and (7,R) cosine eigenforms respectively.

In all three cases of instability for wheel type A, the pair of doublet modes identified will experience strong structural coupling in addition to strong frictional coupling in the case of high longitudinal creepage at the wheel-rail contact. This most likely facilitates the necessary exchange of energy if the instability could indeed be attributed to mode-coupling instability.

It is evident from Figure 14(b) that both the (6,R) and (2,C) doublet mode pairs of wheel type B experience strong structural coupling between the sine and cosine eigenforms as indicated by the sharp rise in the vertical/longitudinal cross receptance at these frequencies. Given that the instability

for wheel type B manifests itself at a frequency halfway between the closely spaced (6,R) and (2,C) modes and that both doublet mode pairs experience strong frictional and structural coupling, it is likely that all four eigenforms couple to create the instability for wheel type B. That is if the instability could indeed be attributed to mode-coupling instability.

Finite Element Modal Analysis

Similar to a loudspeaker membrane the wheel web forms a disk that radiates noise very efficiently when vibrating in a form normal to its plane. Wheel modes having a significant out-of-plane vibration generate the main part of curve squealing. To ascertain that the identified radial and circumferential modes would indeed be capable of the high noise levels associated with squeal occurring in the test curves, it is necessary to verify that these mode shapes have significant out-of-plane wheel web displacement.

The mode shapes of the five eigenfrequencies identified from the previous analysis to be relevant to squeal were calculated (for wheel types A and B) using commercial finite element software. A single flexible wheel was modelled using axi-symmetric finite elements and rigidly constrained at the inner edge of the hub. Omission of the axle results in negligible errors for mode shapes with $n \geq 2$.[2] The material data used for the analysis has a Young's Modulus of 210 GPa, a Poisson's ratio of 0.3 and a density of 7850 kg/m^3.

The deformation of the cross-section for wheel types A and B for the modes identified to be relevant to squeal is presented in Figure 15. The un-deformed shape is shown by the dashed lines in the figure. It is evident from the deformed cross-sections that the radial and circumferential modes for both wheel types A and B contain considerable coupled axial motion of the web. This confirms that the identified modeshapes are capable of emitting high sound pressures.
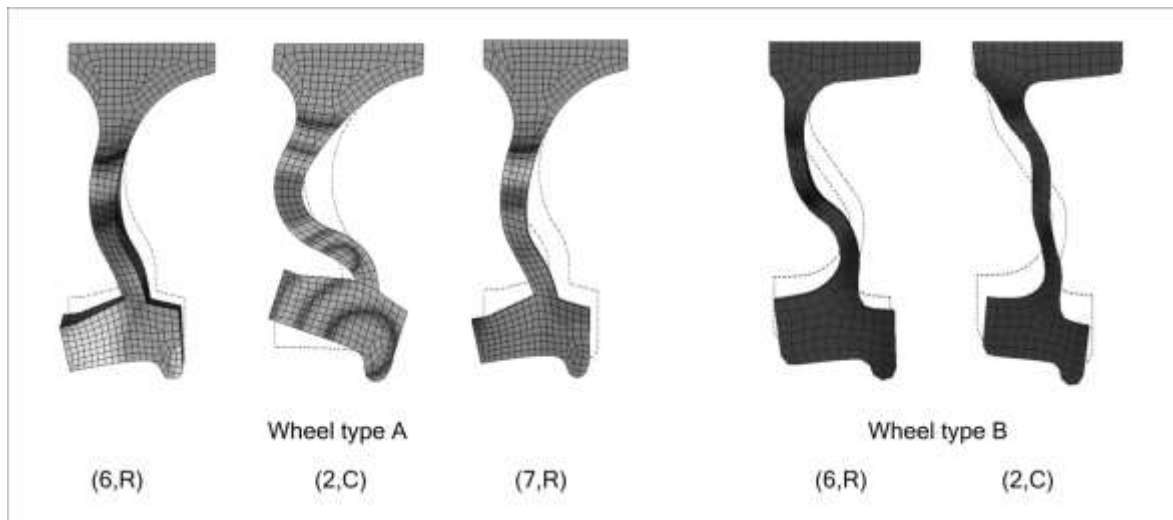
Figure 15. Modes of vibration of wheel types A and B identified to be relevant to squeal

Conclusion

The study aimed to characterise the phenomenon of squeal occurring in large radius curves with respect to the key kinematic parameters and wheelset dynamics influencing its generation.

The key kinematic parameter identified as influencing squeal in the large radius test curves is lateral displacement of the wheelset leading to high levels of longitudinal creepage at the wheel-rail contact of the squealing wheel. In addition, the squealing wheelsets curved with near zero AoAs leading to little to no lateral creepage at the wheel-rail contact. The longitudinal creepage acting at the contact of the squealing wheels in the analysed cases exceeded 1.2%, which proves the likelihood of creep saturation and subsequently squeal due to unsteady longitudinal creepage to occur in the large radius curves.

The locality of the measured unstable frequency for wheel type B with respect to the closest wheel eigenmodes is characteristic of mode-coupling instability. If mode-coupling instability was to be applied to curve squeal excited as a result of the presence of large longitudinal creepage at the wheel-rail interface, it would suggest that the self-excited oscillations are to be caused by the proportionality between the longitudinal creep force and the normal force during sliding as well as the coupling between the radial and circumferential degrees of freedom of the wheel-rail system with respect to the contact point. In line with the above statement, modal analysis of a mounted wheel revealed that for each unstable frequency, two eigenmodes are likely to be important: one which has a large mode shape component at the wheel-rail contact in the circumferential direction and another which has a large mode shape component at the wheel-rail contact in the radial direction. This proves the existence of strong frictional coupling between the radial and circumferential degrees of freedom in the wheel-rail contact in the presence of high levels of longitudinal creepage at the unstable frequencies. Strong structural coupling between the above pair of modes (with respect to the wheel-

rail contact point) also exist as shown by the contact point vertical/longitudinal cross receptance of a freely suspended wheelset. Based on the above evidence, a frictional self-excitation mechanism based on mode-coupling is favoured as being responsible for squeal excited in the large radius test curves. A model based on this mechanism will be developed in the near future.

Results from the finite element modal analysis have verified that radial and circumferential modes identified to be relevant to squeal are indeed capable of high sound emission due to significant out-of-plane displacement of the wheel web.

In contrast to the state of the current knowledge not considering longitudinal creepage relevant to squeal, the results of this research prove the importance of longitudinal creepage as a mechanism for curve squeal. The research further also opens up the relevancy of mode-coupling instability to curve squeal and provide the necessary data to validate a model based mode-coupling instability.

References

1. Fourie DJ. *Mechanisms influencing railway wheel squeal generation in large radius curves.* Master's Thesis, University of Johannesburg, South Africa, 2011.

2. Thompson DJ. *Railway noise and vibration: mechanisms, modelling and means of control.* 1st ed. Oxford: Elsevier, 2009.

3. Vincent M, et al. Curve squealing of urban rolling stock – Part 1: State of the art and field measurements. *J Sound Vib* 2006; 293: 691-700.

4. Pieringer A. A numerical investigation of curve squeal in the case of constant wheel/rail friction. *J Sound Vib* 2014; 333: 4295-4313.

5. Rudd MJ. Wheel/rail noise – Part II: Wheel squeal. *J Sound Vib* 1976; 46.3: 381-394.

6. Periard FJ. *Wheel-rail noise generation: Curve squealing by trams.* PhD Thesis, Delft University of Technology, Netherlands, 1998.

7. Heckl MA and Abrahams ID. Curve squeal of train wheels, Part 1: Mathematical model for its generation. *J Sound Vib* 2000; 229: 695-707.

8. De Beer FG, Janssens MHA and Kooijman PP. Squeal noise of rail-bound vehicles influenced by lateral contact position. *J Sound Vib* 2003; 267: 497-507.

9. Chiello O, et al. Curve squealing of urban rolling stock – Part 3: Theoretical model. *J Sound Vib* 2006; 293: 710-727.

10. Glocker C, Cataldi-Spinola E and Leine RI. Curve squealing of trains: Measurement, modelling and simulation. *J Sound Vib* 2009; 324: 695-702.

11. Jiang J, Dwight R and Anderson D. Field verification of curving noise mechanisms. In: Maeda T, et al. (eds) *Noise and Vibration Mitigation for Rail Transportation Systems: Proceedings of the 10th International Workshop on Railway Noise, Nagahama, Japan, 18-22 October 2010.* Japan: Springer, 2012, pp.349-356.

12. Curley D, et al. Field trials of gauge face lubrication and top of rail friction modification for curve noise mitigation. In: *Proceedings of the 11th International Workshop on Railway Noise*, Uddevalla, Sweden, 9-13 September 2013, pp.511-518. Uddevalla: Chalmers University of Technology.

13. Jiang J, Anderson D and Dwight R. The mechanisms of curve squeal. In: *Proceedings* curve. In: Schulte-Wenning B, et al. (eds) *Noise and Vibration Mitigation for Rail Transportation Systems: Proceedings of the 9th International Workshop on Railway Noise, Munich, Germany, 4-8 September 2007.* Berlin, Heidelberg: Springer, 2008, pp.313-319.

14. Thompson DJ and Monk-Steel AD. *A Theoretical model for curve squeal.* Report for UIC project Curve Squeal. Institute of Sound and Vibration Research, University of Southampton, UK, 23 February 2003.

15. Huang ZY, Thompson DJ and Jones CJC. Squeal prediction for a bogied vehicle in a curve. In: *Proceedings of the 11th International Workshop on Railway Noise*, Uddevalla, Sweden, 9-13 September 2013, pp.655-662. Uddevalla: Chalmers University of Technology.

16. Grassie SL and Kalousek J. Rail corrugations: Characteristics, causes and treatments. *J Rail and Rapid Transit* 1993; 207.1: 57-68.

17. Transportation Technology Center, INC. (TTCI), *Vertical and Lateral Force Measuring Circuit, Installation Information.* Pueblo: TTCI, June 2010.

18. Stefanelli R, Dual J and Cataldi-Spinola E. Acoustic modelling of railway wheels and acoustic measurements to determine involved eigenmodes in the curve squealing phenomenon. *J Vehicle System Dynamics* 2006; 44: 286-295.

19. Kik W. AcRadSchiene Version 4.4, *To create or approximate wheel/rail profiles*. Berlin: ArgeCare, 2010.

20. Kerr M, et al. Squeal appeal: Addressing noise at the wheel/rail interface. In: *Proceedings of Conference on Railway Engineering,* Rockhampton, Australia, 7-9 September 1998, pp.317-324. Queensland: Central Queensland University.

21. International Heavy Haul Association (IHHA). *Guidelines to best practises for heavy haul railway operations: Wheel and rail interface issues.* Virginia:IHHA, May 2001.

22. Monk-Steel AD, et al. An investigation into the influence of longitudinal creepage on railway squeal noise due to lateral creepage. *J Sound Vib* 2006; 293: 766-776.

23. Hoffmann N, et al. A minimal model for studying properties of the mode-coupling type instability in friction induced oscillations. *Mechanics Research Communications* 2002; 29: 197-205.